Simulation of Aluminum nanoparticles formation by femtosecond laser ablation in water Ambient

Ahmed Obaid Soary and Munther B. Hassan
Physics Department, Faculty of Science, University of Kufa, Najaf, Iraq.
Email : ahmed.alkillabi@uokufa.edu.iq

Abstract

Formation of Aluminum (Al) Nanoparticles in water by femtosecond laser ablation is studied numerically by considering the effect of femtosecond laser parameters, target and liquid properties. The absorption of laser energy by Aluminum is simulated using Single-Temperature Model (STM) and results obtained from this model are compared with experimental studies. Classical Nucleation Theory is used to calculate free-energy of critical clusters production and size distribution of nanoparticles (NPs) as function of laser energy and pulse duration in femtosecond range by considering concentration and delay time during the laser generated plume expansion in liquid. Finally, we deduce and point the optimum condition for the growth of Aluminum NPs of desired size and dispersion using STM.

Keywords: Pulsed laser ablation in liquid, ultra-short laser-metal interaction, aluminum nanoparticles, nucleation.

الخلاصة

اجرينا دراسة عددية لانتاج جسيمات الألمنيوم النانوية في الماء بطريقة الإستئصال بليزرِ الفمتوسكند بإعتبار تأثيرِ معاملات ليزرِ الفمتوسكند، خواص الهدف وخواص السائل. كما عملنا محاكات حاسوبية لعملية امتصاص طاقة الليزرِ من قبل الألمنيوم بإستعمال نموذج درجة حرارة الواحدة (STM) وقورنت النَتائِج المستحصلة مِنْ هذا النموذجِ بالدِراسات التجريبية. كذلك استخدمت نظرية التنوية الكلاسيكية لحِساب الطاقة الحرة اللازمة لإنتاج العناقيد الحرجة ولحساب التوزيع الحجمِي للجسيمات النانوية كدالة لطاقة الليزرِ وزمن النبضة في مدى الفمتوسكند مع الاخذ بنظر الاعتِبار تاثير التركيزِ وزمن تأخيرِ عمود البلازما المتوسع في السائل والمتكون بواسطة قصف الهدف بالليزرِ. أخيراً، استنتجنا و حددنا الضرف الامثل لنمو جسيمات ألالمنيوم النانوية بالاحجام المرغوبة والتفرّق الافضل باستعمال نموذج درجة الحرارة الواحدة.

1. Introduction

Nanoparticles (NPs) exhibit superior physical, chemical and optical properties, therefore, find extensive use in various physical, biological, biomedical applications.These include solar cells [1], sensor [2], photo-thermal therapy [3], cooling system [4], nanophotonics devices [5], catalysis [6], carrier systems for drug delivery [7], optoelectronic device [8], cancer treatment [9,10], imaging, sensing, biology and medicine [11]. Laser-generated nanoparticles have also found many applications in bio-photonics, medicine and in the development of photovoltaic cells. Many experiments have been performed demonstrating the formation of these particles from solid targets in vacuum, in the presence of a gas or a liquid; however, it is still difficult to predict the size distribution of these particles. The efforts of many researchers have focused on obtaining smaller size NPs and narrower size dispersion [12-14]. There is large number of factors which affect the final size distribution; the crucial factor for the formation of narrow size distribution is careful selection of laser parameters such as pulse duration, laser fluence, and repetition rate. Target

material Properties affect absorption and the ablated material quantity, thus affecting the plasma plume parameters, and liquid properties such as temperature, mechanical impedance, and viscosity which play a role in shock wave and cavitations bubble formation. In particular, it has been confirmed that lower laser fluence [15] and smaller laser beam size [16] are useful for the formation of the smaller nanoparticles.

To understand the mechanism of nanoparticles formation by pulse laser ablation, detailed study of the material evaporation–condensation process is required. Several analytical approaches have been used to study this process, such as the statistical model of Rice, Ramsperger and Kassel (RRK) [17,18] and classical nucleation theory (CNT) [19,20]. Molecular dynamics (MD) methods [20- 22] have been used for investigation of the evaporation process or the formation and evolution processes of clusters of many materials. Several MD simulations [234,24] and experiments [25-27] of laser ablation of solids have shown that clusters are formed in the expanding ablation plume. Theoretical studies of the ultrashort laser absorption by metals using two-temperature model (TTM) have been reported by several researchers [28-30]. Conduction band electrons absorb laser energy and then diffuse it inside the target material due to their thermal conductivity, where the lattice is simultaneously heated by electron-phonon coupling. In fact, numerical solutions turned out to be sensitive to a number of governing parameters, such as electron-phonon collisions rate, thermal conductivity coefficient, and optical absorption depth; which in turn may be function of temperature and density to accurately determine these coefficients in simulation of ultrashort laser-material interaction. [31, 32].

Using TTM for shorter fs laser irradiation of metal the temperature of lattice remains at room temperature for long time (a few ps) especially if the metal has a large heat capacity, thus to achieve more accurate results we propose use of single-temperature model STM in this work. In STM, the energy absorption takes place during fs-pulse interaction with solids and energy transfer to the lattice takes place when the laser pulse is OFF [33]. The difference between Two Temperature Model (TTM) and Single Temperature Model (STM) is that during the time when the laser pulse is ON, the electron-lattice coupling in STM can be neglected, and the lattice temperature is due to transfer of energy from maximum electron temperature. Therefore, STM is suitable for fs-pulse duration because it considers the maximum energy of excited electrons as an energy source for lattice heating without dependence of electrons-lattice coupling.

2. Theory

2.1 Absorption

In Two Temperature Model (TTM) the absorption of laser light takes place by the conduction band electrons and subsequently the energy diffuses inside the material from excited electrons to lattice after the electrons acquire very high temperature ~10^3K. This increasing lattice temperature largely depends on electron-phonon coupling, electron relaxation time and heat capacity of material. For shorter fs-laser pulse, therefore, the increase in lattice temperature is insignificant during laser pulse duration and very significant after end of the laser pulse for a few ps[34,35]. The two-temperature diffusion model can be described by the following one-dimensional equations;

$$C_e \frac{\partial T_e}{\partial t} = -\frac{\partial Q(z)}{\partial z} - \gamma(T_e - T_i) + S \qquad (1)$$

$$C_i \frac{\partial T_i}{\partial t} = \gamma(T_e - T_i) \qquad (2)$$

$$Q(z) = -k_e \frac{\partial T_e}{\partial z}, \quad S = I(t) A\alpha \exp(-\alpha z) \qquad (3)$$

where, T_e and T_i are the electron and the lattice temperatures. $Q(z)$ is the heat flux, S is the laser heating source term, C_e and C_i are the electron and lattice heat capacities per unit volume, respectively. γ is the electron-phonon coupling coefficient, k_e and k_i are the electron and lattice thermal conductivity, respectively, $k_e=k_o(T_e)(T_e/T_i)$ where $k_o(T_e)$ is the conventional equilibrium thermal conductivity of the metal. $I(t)$ is the laser intensity measured in [W·cm^{-2}], α is the material absorption coefficient including the surface absorptivity, A is the surface transmissivity. There are three very important characteristic time scales in these equations: τ_e, τ_i and τ_L, where $\tau_e = C_e/\gamma$ is the electron cooling time, $\tau_i = C_i/\gamma$ is the lattice heating time ($\tau_e << \tau_i$) and τ_L is the laser pulse duration. These parameters define femtosecond, picosecond and nanosecond regimes of the laser-metal interaction.

In case of fs-pulse interaction with material, pulse width is much smaller than the electron cooling time i.e. $\tau_L << \tau_e$, therefore, during the time when the laser pulse is ON, the electron lattice coupling can be neglected, and the electron conduction term is very small, Eqs. (1) and (2) are reduced to a single equation given by[35]

$$C_e' \frac{\partial T_e^2}{\partial t} = 2 I_O \alpha A \exp(\alpha z) \qquad (4)$$

which on integration gives,

$$T_e(t) = \{T_O^2 + \frac{2 I_O \alpha A}{C_e'} t e^{-\alpha z}\}^{1/2} \qquad (5)$$

$$T_e(\tau_L) \approx (\frac{2 I_O \tau_L \alpha}{C_e'})^{1/2} \exp(-\frac{z}{\delta}) \qquad (6)$$

where $T_o=T_e(0)$ is the initial temperature of the electrons and I_0 is the incident laser power density. At the end of laser pulse, the electrons will attain maximum energy and the thermal conduction to the lattice in fs time scale is neglected, the temperature of the electron is,

$$T_e(\tau_L) \approx \left(\frac{2 I_O \tau_L \alpha}{C_e'} \right)^{1/2} \exp(-\frac{z}{\delta}) \qquad (7)$$

The electron temperature is much greater than the ambient temperature $Te(\tau_L) >> T_o$ and we assume that the absorption of the laser energy only up to skin depth $\delta(=2/\alpha)$. The electron temperature attains a maximum value during the laser pulse followed by rapid transfer of energy to the lattice after the laser pulse. Thus, the electrons will be cooled with rapid rate and the temperature of lattice T_i will be increased, therefore using Eq. 2 we can get T_i as:

$$T_i = \frac{F_a \alpha}{C_i} e^{-\alpha z} \qquad (8)$$

The condition for evaporation of the target material will be fulfilled if the absorbed energy exceeds the specific heat of vaporization, i.e. when $C_i T_i > \rho \Omega$, where ρ is the density and Ω is the specific heat of evaporation per unit mass. [35]

Using STM, we consider that there are two independent and consequent steps for energy transfer, the first is from laser to electrons and the second is from electrons to lattice when electrons temperature reach to maximum energy. Therefore, by using STM we expect that the energy of the excited electrons to be larger and consequently higher rate of lattice heating compared to TTM.

2.2 Nucleation

Now, after calculating the amount of laser energy absorbed by Aluminum target and the electrons and lattice temperatures using both TTM and STM for the same bulk values and the laser parameters, we now study the nucleation process of NPs within the induced plasma plume inside the liquid (water in this study). By modeling the free energy ΔG of the growing embryos (or nuclei which serve as monomers for the primary-particle nucleation as solutes) which consist of number (n) of ablated species (atoms, ions, molecules), we can calculate the critical clusters n_c and the rate of production of critical clusters ρ(t) from the calculation of critical free energy ΔG_c.

During fs-laser pulse, laser energy absorbed by the electrons and subsequent relaxation of energy to the target material leads to the generation of heat waves followed by the generation of two shock waves propagating (inside and outside the target) [36]. The formation rate of critical nuclei, per unit volume ($m^{-3}\sec^{-1}$), can be written as:

$$\rho(t) = 4\pi a n_c^{1/3} D c^2 e^{-\Delta G_C / KT} \qquad (9)$$

where, a is the effective radius of plume species (Aluminum atoms =1.43 x 10^{-10}m), D is the diffusion coefficient of Aluminum atoms in water ($m^2\sec^{-1}$), n_c is number of solutes in an embryo at the critical nucleus size, ΔG is the free energy of the growing embryos, considering the solute concentration c(t), at time t, is larger than their equilibrium saturation concentration c_O.In case of $n < n_c$ (embryos of size smaller than critical embryos), the attaching and detaching processes into or from embryo can occur, so that the size distribution is given by the equilibrium form. Thus, when the embryos sizes are reaching to critical size of n_c, the exponential term in Eq. (9) is considered as a factor of thermodynamic distribution. While for sizes equal or larger than n_c, we can assume fully irreversible dynamics, It is assumed that the radius of nuclei collection (cluster) equal to $an^{1/3}$, where a is the effective solute radius, ($n^{1/3)}$ is the volume filling-fraction correction [37].
For n-embryos the free energy can be written as:

$$G(n) = -nKT \ln\left(\frac{c}{c_o}\right) + 4\pi a^2 n^{2/3}\sigma \qquad (10)$$

which involves the bulk term, proportional to n, and the surface term proportional to $n^{2/3}$.
To calculate ΔG_c we will ignore $G(1)$ because it is much smaller than ΔG_c of large n, the significant factors in this equation are the surface tension and the concentration of solutes $c(t)$, where both n_c and ΔG_c are functions of $c(t)$. We can calculate the critical value n_c from $\partial G/\partial n = 0$, then,

$$n_c = [8\pi a^2\sigma / 3\mathrm{KT}\ln(c/c_o)]^3 \qquad (11)$$

And $$\Delta G_C = \frac{256\pi^3 a^6 \sigma^3}{27(KT)^2(\ln c/c_o)^2} \qquad (12)$$

The value of the effective surface tension of nanosize Aluminum embryos is $\sigma \approx 0.84$ N/m, the saturation concentration of Aluminum in solution is $c_o = 1.6\times10^{15}$ m^{-3} [38], and $c(t)$ changes with time and it decreases by the formation and then the growth of critical nuclei. If the process is considered as an irreversible formation, thus, we write

$$dc/dt = -n_c\rho(t) \qquad (13)$$

Where, the initial concentration of the Aluminum solution is $c(0) = 6.2 \times 10^{25}m^{-3}$ [37]. Using Eqs. (9) to (12) we get following equations for $c(t)$ and $\rho(t)$

$$\frac{dc}{dt} = -\frac{2^{14}\pi^5 a^9 \sigma^4 D\ c^2}{(3KT)^4[\ln(c/c_o)]^4}\exp\left\{-\frac{2^8\pi^3 a^6\sigma^3}{(3KT)^3[\ln(c/c_o)]^2}\right\} \quad (14)$$

$$\rho(t) = \frac{2^5\pi^2 a^3\sigma\ D\ c^2}{3KT\ \ln(c/c_o)}\exp\left\{-\frac{2^8\pi^3 a^6\sigma^3}{(3KT)^3[\ln(c/c_o)]^2}\right\} \quad (15)$$

After plasma plume generation by fs-laser, we consider that the generated plasma plume does not absorb laser radiation. In this case, a larger fraction of energy is transferred into the target, so that the laser intensity which is required to create plasma plume with length L(t) and pressure P(t) can be written as:

$$I(t) = P(t)\frac{dL(t)}{dt} + \frac{d[(1-\alpha)E_i(t)L(t)]}{dt} \quad (16)$$

where, $E_i(t)$ is the internal energy of the created plasma; equal to sum of thermal and ionization energy $E_i = E_{th} + E_{ion}$, where $E_{th} = \alpha E_i$ and $E_{ion} = (1-\alpha)E_i$, in case of fs-laser as described above, E_{th} is nearly zero and α determines the energy fraction transferred to the thermal energy of the plume. We can solve this equation using the ideal gas assumption to obtain the initial pressure of the plasma plume:

$$P_O = P(\tau) = \sqrt{\frac{\alpha}{2\alpha+3}ZI_O} \quad (17)$$

here, Z refers to combined shock impedance defined as [37].

$$\frac{2}{Z} = \frac{1}{Z_{Al}} + \frac{1}{Z_{Water}} \quad (18)$$

Z_{Al} is defined as the product of the density and shock velocity $Z_{Al}=\rho_{Al}U_{Al}$, where ρ is the density of Al (=2.37 g·cm^{-3}) and U is the shock velocity (=5,000 m·s^{-1}). Z_{Al} and Z_{water} are (11.85 x10^5 and 1.65x10^5 g/s.cm^2), respectively [37]. Then Z=19.55x 10^5 g/s.cm^2, So that the pressure $P(\tau)$ and temperature $T_2 = T_1(\frac{P_2}{P_1})^{\frac{\gamma-1}{\gamma}}$ are depending also on pulse duration, where γ is the adiabatic parameter, $\gamma = \frac{1+2\alpha}{3}$.

It can be noticed from Eqs. (17) and (18) that the initial plume length is smaller, whereas the initial pressure is larger for fs-laser pulses than for longer laser pulses. After that the generated plasma plume will expand adiabatically behind the shock wave. Using the common equations for the adiabatic expansion we can obtain expressions for pressure length of expanded plasma as a function of time [36],

$$P(t) = P_O\left[1+\frac{\gamma+1}{\tau}(t-\tau)\right]^{-\gamma/\gamma+1} \quad (19)$$

$$L(t) = L_O\left[1+\frac{\gamma+1}{\tau}(t-\tau)\right]^{1/\gamma+1} \quad (20)$$

From these equations, the higher value of plume number density may be evaluated in this stage (growth stage), whereas in the case of shorter pulses the plume temperature is smaller, that will lead to formation of NPs with smaller size (smaller primary particles), whose free energy controls the size of NPs according to Eq. (10).

In this stage of primary particle growth we can study several cases considering the following: If the temperature of plasma still high after laser pulse, the evaporation process will

increase the number density of primary particle while there is a decrease of the density due to the growth of primary particles by adding both monomer and cluster. If the temperature of both clusters and plasma is not too high, this process will overcome evaporation that appears in case of fs-laser more than others. These clusters can be considered as seeds for the following much longer process i.e. formation of large NPs by aggregation of primary particles or clusters occurs. The aggregation stage takes place after growth stage of primary particles, where the rates of formation of large NPs can be determined in this stage, thus the time-evolution of cluster can be described in this stage by simplified master equations.

For evolution population of NPs we consider that the size of cluster can be defined by the number (*s*) of primary particles (singlets), which were aggregated into each secondary particle, where *s* refers to this number *s* = 1, 2, 3,.... , thus we can write $N_1,N_2,N_3,...$ to refer to the population of cluster with one, two, three ,.... primary particle(s). By keeping in mind the fact that clusters can take or give singlets particles, then the population of cluster of s-primary particles will change during the time of the process, in this case of particles growth the population of NPs can be describe by master equation, all these populations are fed by critical clusters , the rate of production of critical clusters at this stage is given by Eq. (9) where the initial parameters of the solution, such as temperature, concentration of solute, particle size, and density, are very important functions to determine the critical cluster size, its production rate, and further evolution of NPs.

For the singlet population, the equation of its concentration can be obtained using the rate of the primary particle formation, ρ (t) and the rate of its transformations.

$$\frac{dN_1}{dt} = \rho(t) - \sum_{j=2}^{\infty} j \frac{dN_j}{dt} \qquad (21)$$

with the initial values $N_s(0) = 0$ for all *s* =1, 2, 3, ...
The concentrations of dimers is given by,

$$\frac{dN_2}{dt} = fk_1N_1^2 - k_2N_1N_2 \qquad (22)$$

where, the factor f = 1/2 for the monomer-monomer aggregation term due to the double counting, thus it is only for the clusters of *s*=2[37]. The population of other larger clusters is given by:

$$\frac{dN_s}{dt} = k_{s-1}N_1N_{s-1} - k_2N_1N_s \qquad (23)$$

where, K_s is the attachment rate constant, which can be described by Smoluchowski rate expression [39],

$$K_s = 4\pi(R_1 + R_s)(D_1 + D_s) \qquad (24)$$

but can be used simplification of Park-Privman [37] by ignoring the cluster-cluster aggregations because this process is slower than singlet-cluster aggregations process, resulting from that they have larger diffusion constants (D_1), thus k_s may be written as:

$$K_s = 4\pi R_s D_1 \qquad (25)$$

where, R_s is the radius of the s-singlet particles, given by $R_s = 1.2\, r\, s^{1/3}$, *r* and D_1 are the average radius and diffusion coefficient of the primary particles, respectively.

The solute diffusion coefficient *D* can be estimated by using the Stokes-Einstein formula for diffusion of spherical particles through liquid with actual radius of the Aluminum atom [40],

$$D = \frac{k_B T}{6\pi\eta r} \qquad (26)$$

Here η is viscosity of water (kg/m.sec) $\eta=A*10^{B/(T-C)}$, A = 2.414 *10^{-5}Pa s; B =247.8 K; and C = 140 K.[36,40]. We can estimate the yield of clusters using Eqs.(21-23), using approximation (i) ignoring the cluster-cluster aggregations as referred above, (ii) the radius of the captured primary particles close to the critical radius and (iii) the size of critical nuclei do not increase before its attachment to the secondary particles.

3. Results and Discussion

In this work, we have considered the absorption of fs-laser beam by Aluminum target immersed in water using both single temperature model (STM) and the two temperature model (TTM). The temperature at the surface of Aluminum target, calculated from Eqs. (1) and (2) for TTM, and from Eqs. (7) and (8) for STM, shows that during 100 ps after fs-laser pulse, the lattice temperature reaches to $3x10^3$ K in case of TTM and to $7x10^3$ K in case of STM, as shown in Fig. 2 and 3. In order to explain the difference in results obtained from STM and TTM simulations, it should be emphasized that the electron-phonon coupling greatly influences the energy transfer between the electrons and the lattice and thus affects the temperature rise of both electrons and lattice in case of STM. Ignoring this term allows electrons temperature to rise without losing part of their energy to the lattice, only if this temperature reach to a maximum value, the electrons will then be a new source of lattice heating. If we considered the electron-electron collision τ_{ee}=1-10 fs, the electron relaxation time τ_{ep} 0.1-1 ps [41], the result of TTM in Fig. 2 is in agreement with our expectation. While in case of STM after the end of pulse duration (100 fs) the electrons temperature reaches to a maximum value $2x10^4$ K (see Fig. 2), at this time the lattice will get the energy from electrons. The temperature deference between T_e and T_l (about $7x10^3$) in case of STM as shown in Fig. 2 and 3, is due to the difference in values of volumetric specific heat of electrons (=$1.065x10^3$ J/m^3 K^2)[35] and lattice (=$8x10^3$ J/m^3 K^2)[42].

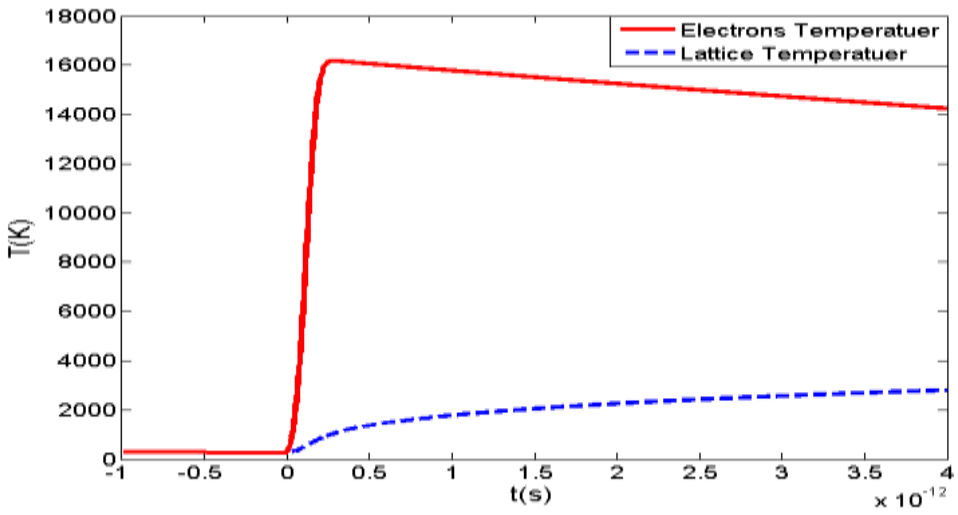

Figure 2: Two-temperature model for Aluminum target at surface during 5 ps, the pulse duration and fluence of laser are 100fs and 0.6 J/cm^2.

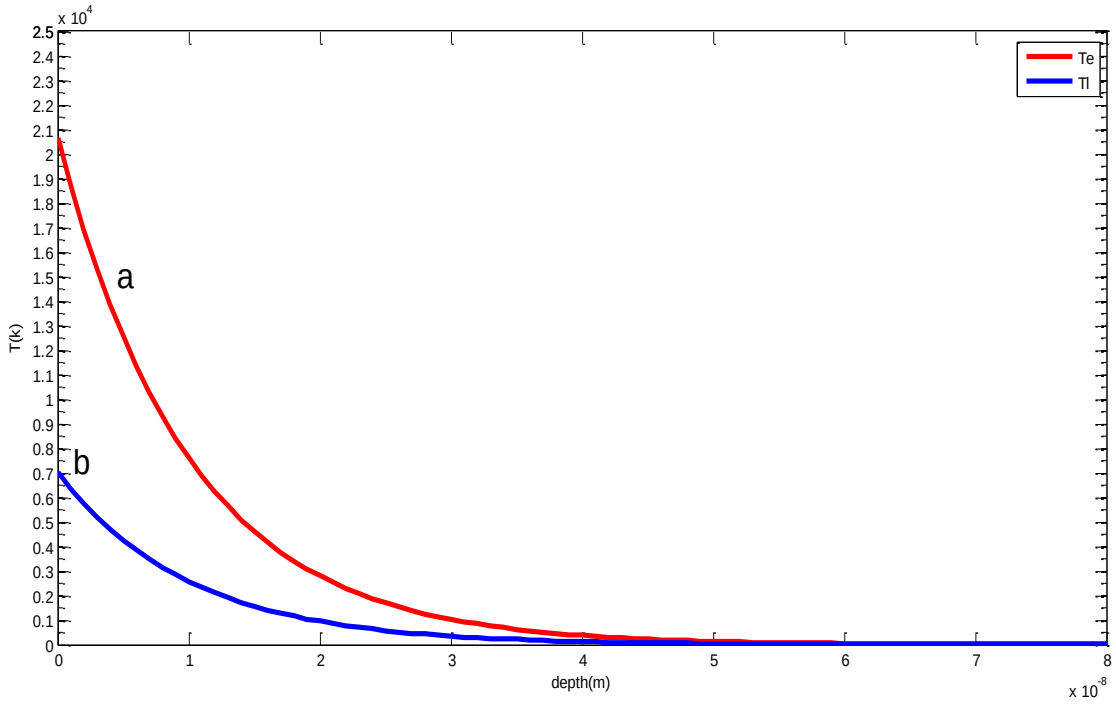

Figure 3: Calculated maximum electrons temperature (a) and lattice temperature (b) by Single-temperature model for a Aluminum target. The pulse duration and fluence of laser are 100fs and 0.6 J/cm^2, respectively.

By solving Eq. (10) for the case of $\partial G/\partial n$ =0, the results plotted in Fig. 4 show free energy at several temperatures and critical particles sizes n_c at different temperature for both TTM and STM. We found that there is a clear deference between the results obtained from the two models; in both cases the increasing temperature result in decreasing sizes and the sizes of critical particles are smaller in case of STM. This can be explained by Eq. (10),where the bulk term is proportional to the particles temperature.

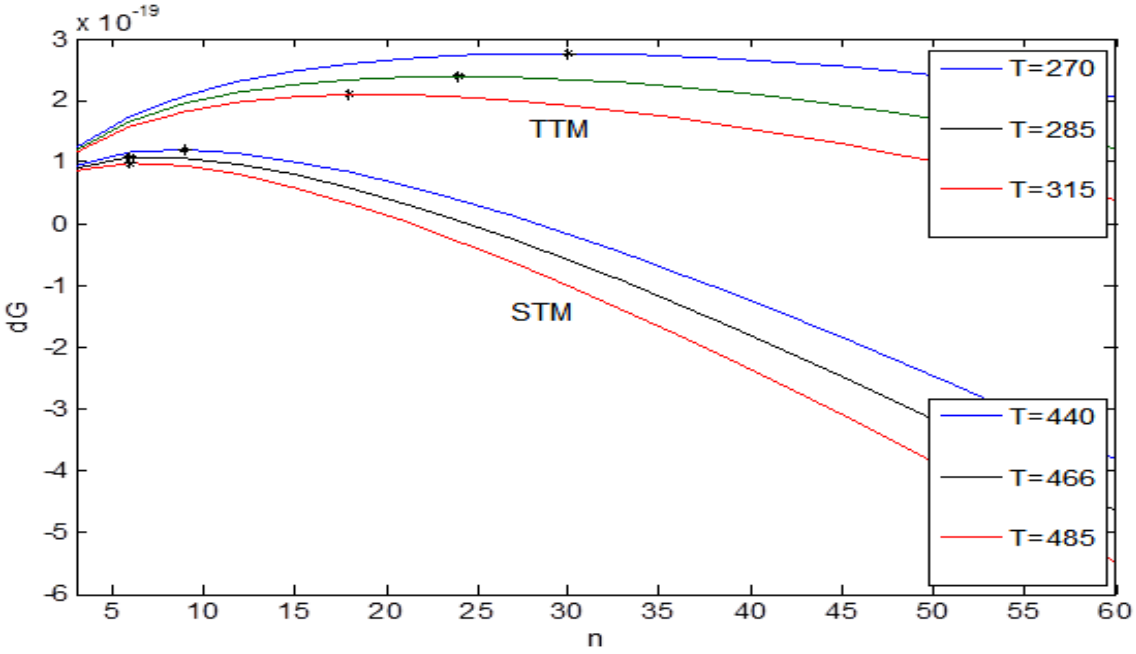

Figure 4: Free energy of production of critical particles in case of TTM (upper) and in case of STM (lower) at different temperatures.

It should be mentioned that the cooling rate of ablated species in solution has an important role in the growth of particles to the critical size, we expect that this critical size will increase with the increasing deference in temperatures between the ablated species and the solution i.e. the cooling rate in STM is much higher than in TTM, this is confirmed by the results of free energy in Fig. 4, although this will lead to smaller clusters size and narrow dispersion. The high temperature in case of STM will lead to continuous aggregations to produce larger clusters over longer times (≈100 μs) thus increasing NPs size with a wide dispersion. The deference between TTM and STM results is shown in Fig. 5 and Fig. 6, where it can be noticed that the dispersion is narrower in case of TTM, and the best dispersion is in the range 9 -15 nm at 340 K, while in case of STM there is clearly large dispersion with increasing temperatures.

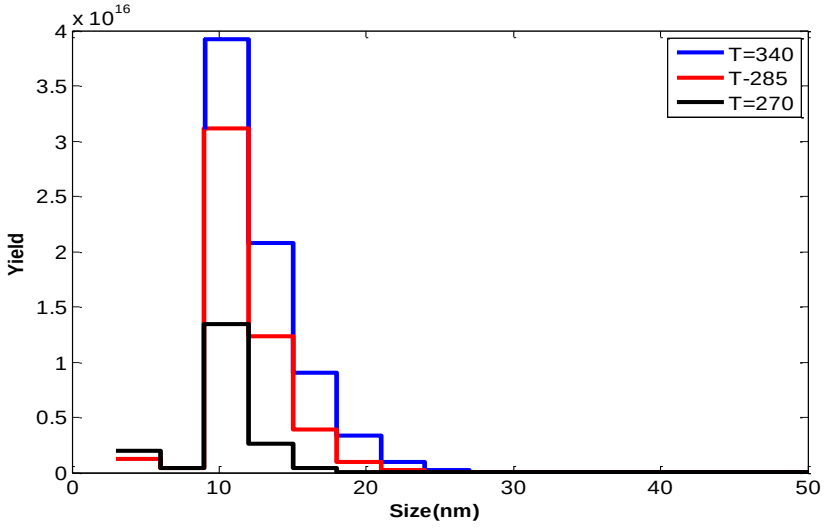

Figure 5: Size distribution of Aluminum NPs at different solution temperatures in case of TTM .

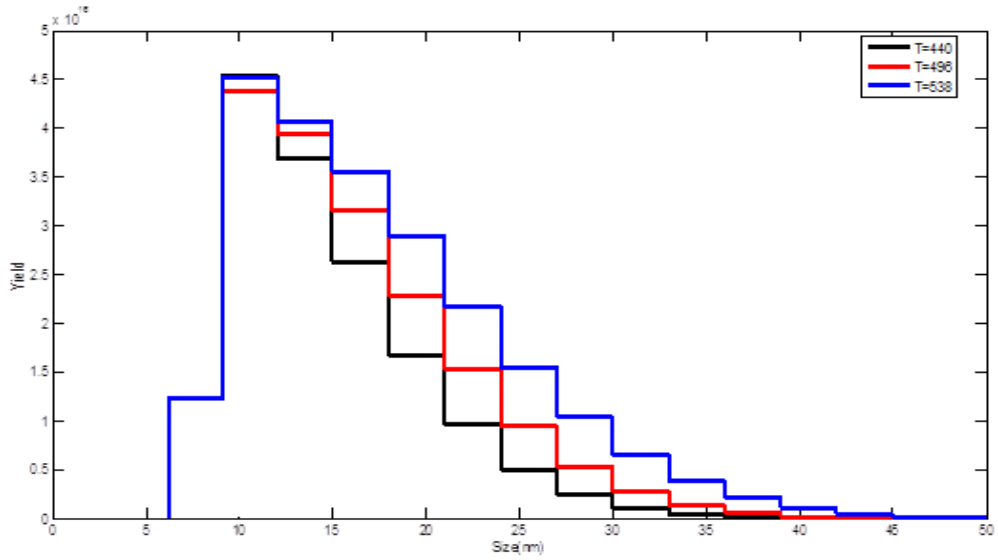

Figure 6: Size distribution of Aluminum NPs at different solution temperatures in case of STM.

Also, the size and the dispersion of nanoparticles depend on the concentration of solutes (inside the solution) and the initial plume pressure p_o, which depends on laser power density I_o and the parameters of both of target material and the ambient (water) given by Eq.(17), for pressure and temperature evolution in expanding plume we used Eq.(18).

The adiabatically expanding plasma plume with high temperature of clusters leads to production of large size nanoparticles because the large clusters have larger collision cross section than the smaller clusters and the primary particles, we expect that is effective in case of increasing volume of plume. Furthermore, the effect of delay times (0.01μs,1μs and 5μs) on the nanoparticles size distribution is shown in Fig. 7, where the size distribution and the dispersion increase with increasing delay time at temperature (685K), these results are in good agreement with the previous experimental results [13,14], and theoretical calculations [43,44].

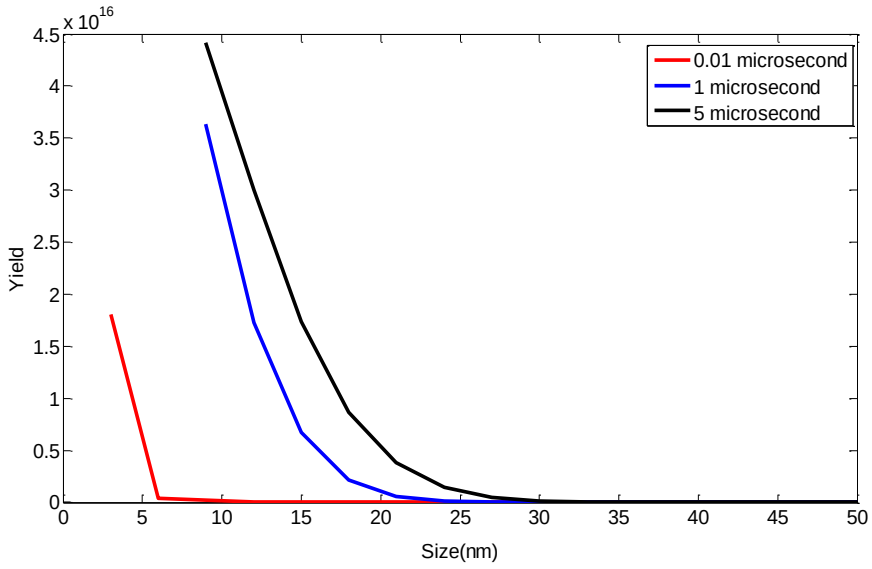

Figure 7: Calculated size distribution of Aluminum NPs for delay time 0.01μs, 1μs and 5μs after generation of plasma plume using nucleation theory.

4. Summary

The simulation results obtained from the absorption of laser energy by Aluminum target in water suggest that the ablated species acquire higher temperature in case of STM, this lead to formation of larger NPs sizes, in spite of high cooling rates and small critical particles sizes, due to continuing aggregation processes over longer time For shorter plasma plume expansion times (< 0.01μs), the obtained results are better. We conclude that in case of STM the best results are obtained when the temperature is lower but enough to obtain high cooling rates and small critical particles sizes. We believe that the growth of large clusters can be reduced and STM will be suitable to simulate the femtosecond laser absorption at lower fluence (< 0.6 to 0.01 J/cm^2) in materials with higher heat capacity, this is a subject of our next study.

References

[1] Tong S W, Zhang C F, Jiang C Y, Liu G, Ling Q D and Kan E T 2008 Chem. Phys. Lett. 453 73.
[2] Shao M, Lu L, Wang H, Luo S and Ma D D 2009 Microchim Acta 164 157.
[3] Rianasari I, Walder L, Burchardt M, Zawisza I, and Wittstock G 2008 ACS journal of surfaces and colloids 24 9110.
[4] Das S K, Choi S U, Yu W and Pradeep T, Nanofluids-Science and Technology, A John Wiley & Sons, INC. Publication (2007).
[5] Prikulis J, Svedberg F, Kal M, 2004 Nano Lett. 4 115.
[6] Sanchez D B, The Surface Plasmon Resonance of Supported Noble Metal Nanoparticles: Characterization, Laser Tailoring, and SERS Application, PhD thesis, Madrid University (2007).
[7] Kabashin A V, Meunier M, Kingston C and Luong J T 2003 J. Phys. Chem. 107 4527.
[8] Arruebo M, Pacheco R F, Ibarra M R, and Santamaria J 2007 Nano Today 2 22.
[9] Mishra M, Kumar H and Tripathi K 2008 Digest J. of Nanomat. and Biostruct. 3 4.
[10]Jain P K, Huang X, El-Sayed I H and El-Sayed M 2008 Am Chem.Soc. Acc. Chem. Res. 41 1578.
[11] Jain P, El-Sayed I H and El-Sayed M 2007 Nano Today 2 18.
[12]Sylvestre J P, Kabashin A V Sacher E and Meunier M 2005 Appl. Phys. A 80 753.
[13] Amoruso S, Ausanio G, Bruzzese R, Gragnaniello L, Lanotte L, Vitiello M and Wang X, 2005 Appl. Surf. Sci. 252 4863.
[14] Amoruso S, Bruzzese R, Vitiello M, Nedialkov N N and Atanasov P A 2005 J. of Appl. Phys. 98 044907.
[15]Mafune F, Kohno J, Takeda Y, Kondow T and Sawabe H J 2001 Phys. Chem. B, 105 5114.
[16]Pyatenko A, Shimokawa K, Yamaguchi M, Nishimura O and Suzuki M 2004 Appl. Phys. A79 803.
[17]Malakhovskii A V and Ben-Zion M 2001 Chem. Phys. 264 135.
[18]Zeifman M I, Garrison B J and Zhigilei L V 2002 J. Appl. Phys. 92 4.
[19] Kinjo T, Ohguchi K, Yasuoka K and Matsumoto M 1999 Comput. Mater. Sci. 14 138.
[20] Schenter G K, Kathmann S M and Garett B C 1999 Phys. Rev. Lett. 82 17.
[21]Frenkel D and Smit B, Understanding Molecular Simulation, Academic Press, 1996.
[22] Zhigilei L V, Kodali P B S and Garrison B J 1997 J. Phys. Chem. B 101 2028; 1998 J. Phys. Chem. B 102 2845.
[23]Zhigilei L V 2003 Appl. Phys. A76 339.
[24] Itina T E, Zhigilei L V and Garrison B J 2002 J. Phys. Chem. 106 303.
[25]Bulgakov A V, Ozerov I and Marine W 2004 Appl. Phys. A79 1591.
[26]Amoruso S, Bruzzese R, Spinelli N. Velotta R, Vitiello M and Wang X 2004 Europhys. Lett.67 404.

[27]Itina T E, Gouriet K, Zhegilei L V, Noel S, Hermann J and Sentis M 2007 Appl. Surf. Sci. 253 7656.
[28]Jiang L and Tsai H 2008 J. of Appl. Phys. 104 093101.
[29]Sonntag S, Roth J, Gaehler F and Trebin H R 2009 Appl. Surf. Sci. 225 9742.
[30]Anisimov S I, Kapeliovich B L and Perel'man T L 1974 Sov. Phys. JEPT, 39 375.
[31] Colombier J P, Combis, P, Bonneau F, Le Harzic R, and Audouard E 2005 Phys. Rev. B71 165406.
[32]Schäfer C, Urbassek H M and Zhigilei L V 2002 Phys. Rev. B 66, 066415.
[33]Chichkov B N, C. Momma, S. Nolte, F. von Alvensleben, A. Tunnermann 1996 Appl. Phys. A63 109.
[34] Ashcroft NW, Mermin N D, Solid State Physics. (Saunders College, Philadelphia, 1976).
[35] Cheng C and Xu X 2005 Phys. Rev. B 72 165415.
[36] Itina T E 2011 J. Phys. Chem. C115, 5044.
[37] Park J, Privman V, and Matijevic´ E, 2001 J. Phys. Chem. B 105, 11630.
[38]Linke, W. F. Solubilities of Inorganic and Metal-Organic Compounds, 4th Ed.; Van Nostrand: Princeton, 1958; Volume 1, page 243.
[39] Ring T A 1991 Powder Technol. 65 195.
[40] Seeton Ch 2006 J. Tribol. Lett. 22 67.
[41] P. Schaaf, Laser Processing of Materials Fundamentals, Applications and Developments, 2010.
[42] Lide D R, CRC Handbook of Chemistry and Physics, 90th Edition, 2009.
[43] Gouriet, K. PhD thesis, Mediterranean University, Marseille, France, 2008.
[44] K. Gouriet, T. E. Itina, S. Noël, J. Hermann, M. Sentis, and L. Zhigilei, Proc. SPIE 7005, 70050T (2008); doi:10.1117/12.782711.